RSC Advances




ROYAL SOCIETY OF CHEMISTRY

www.rsc.org/advances

## Graphical Abstract

**Sulfonated nanohydroxyapatite functionalized with 2-aminoethyl dihydrogen phosphate (HAP@AEPH$_2$-SO$_3$H) as a new recyclable and eco-friendly catalyst for rapid one-pot synthesis of 4,4'-(aryl methylene)bis(3-methyl-1*H*-pyrazol-5-ol)s**

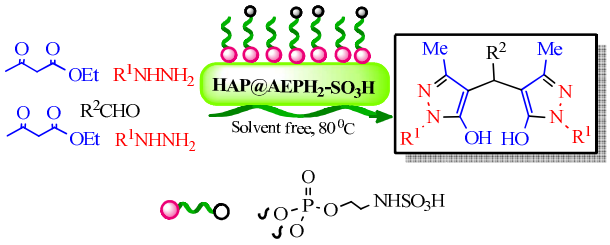


Monireh Zarghani, Batool Akhlaghinia *

HAP@AEPH$_2$-SO$_3$H as a new, green, solid acid catalyst was prepared, characterized and applied for the synthesis of 4,4'-( aryl methylene)bis(3-methyl-1*H*-pyrazol-5-ol)s.

# Sulfonated nanohydroxyapatite functionalized with 2-aminoethyl dihydrogen phosphate (HAP@AEPH$_2$-SO$_3$H) as a new recyclable and eco-friendly catalyst for rapid one-pot synthesis of 4,4'-(aryl methylene)bis(3-methyl-1*H*-pyrazol-5-ol)s

Monireh Zarghani, Batool Akhlaghinia*

**Abstract:** Sulfonated nanohydroxyapatite functionalized with 2-aminoethyl dihydrogen phosphate (HAP@AEPH$_2$-SO$_3$H) as a new green, recyclable solid acid catalyst was prepared and characterized by FT-IR, XRD, SEM, TEM and TGA/DTA techniques. Composition of HAP@AEPH$_2$-SO$_3$H was determined as nonohydroxyapatite, while particles were observed to have nanorods morphology. Size estimations using TEM (10-100 nm) and the crystallinity using XRD (hexagonal phase) are well-matched to character of nanohydroxyapatite. The catalytic activity of HAP@AEPH$_2$-SO$_3$H was evaluated for synthesis of 4,4'-(aryl methylene)bis(3-methyl-1*H*-pyrazol-5-ol)s via one-pot reactions of phenylhydrazine/or hydrazine hydrate, ethylacetoacetate and aldehydes under solvent-free condition. This catalyst showed notable advantages such as environmental friendliness, excellent yields, shorter reaction time, reusability of inexpensive catalyst and easy workup procedure.

**Keywords***:* HAP@AEPH$_2$-SO$_3$H, 4,4'-(aryl methylene)bis(3-methyl-1*H*-pyrazol-5-ol)s, one-pot reaction, green chemistry

## Introduction

4,4′-(Aryl methylene)bis(1*H*-pyrazol-5-ol)s as an important class of heterocyclic compounds have been exhibited a wide range of biological activities such as antimalarial,[1] antifungal,[2] anti-inflammatory,[3] antimicrobial,[4] antinociceptive,[5] antivirals,[6] and antitumor[7] activities. Also, they are used as pesticides,[8] fungicide,[9] analgesic,[10] important intermediates in organic synthesis[11] bis-Schiff bases[12] and ligands.[13] The conventional chemical approach to 4,4′-(aryl methylene)bis(1*H*-pyrazol-5-ol)s derivatives is the reaction of initially formed 3-methyl-5-pyrazolone (from the condensation of hydrazine /aryl hydrazine and ethyl acetoacetate) with aldehydes under a variety of reaction conditions. Xanthan sulfuric acid,[14] phosphomolybdic acid,[15] silica sulfuric acid,[16] 3-aminopropylated silica gel,[17] sodium dodecyl sulfate,[18] tetramethyl-tetra-3,4-pyridinoporphyrazinato copper(II) methyl sulfate,[19] poly(ethylene glycol)-bound sulfonic acid,[20] and others[21-32] can be used as catalysts for this transformation. Catalyst free[33] and electrocatalytic procedure[34] were also used for this preparation. Other methods of preparation include one-pot reactions in which three or more starting materials react together to form a product where all or most of the starting material atoms exist in the final product.[35] In comparison, the one-pot character also, provides some advantages over the classical stepwise synthetic routes such as fewer by-products, lower costs, time, and energy. Recently because of simple purification, excellent synthetic efficiency, atom economy, operational simplicity, elimination of overflow steps and environmental friendliness, one-pot reactions have been paid much attention.[36] Also, one-pot reactions offer formation of complex molecular architectures from simple precursors via formation of several bonds in a simple synthetic operation, without the need for isolation of intermediates.[37] However, a few methods have been reported for the synthesis of these

compounds by one-pot reactions in the presence of silica-bonded *N*-propylpiperazine sulfamic acid (SBPPSA),[38] pyridine trifluoroacetate,[39] *N*,2-dibromo-6-chloro-3,4-dihydro-2*H* benzo[e][1,2,4]thiadiazine-7-sulfonamide 1,1-dioxide (DCDBTSD),[40] ultrasonic irradiation,[41] sulfonated rice husk ash (RHA-$SO_3H$),[42] 2-hydroxy ethylammonium propionate (2-HEAP).[43]

In recent years, to minimize the use and production of hazardous materials, green chemistry encourages chemists to design chemical procedures by using environmentally benign reagents that reduce and prohibit the pollution of nature and ensure perpetual life on the earth.[44] Because of usefulness of one-pot reactions for the synthesis of complex molecules such as drug-like molecules, these kind of reactions play an important role in combinatorial chemistry and industrial chemistry.[45, 46]

Over the past decades, to overcome some problems of homogeneous catalytic processes, heterogeneous catalysts such as mixed metal oxides, zeolites, hydrotalcites, solid-supported catalysts, resins, *etc* are particularly attractive, because of possessing advantages such as ease of separation of product, reusability of the catalyst and improved efficiency. On the other hand, heterogeneous catalysts which has been known for many years has become strategically vital for efficient and ecofriendly organic transformations. Among various heterogeneous catalysts, nanohydroxyapatite (nanoHAP [$Ca_{10}(PO_4)_6(OH)_2$]) as an important inorganic nanomaterial with high surface area and low particle size, provide high biocompatibility, great catalytic activity and good adsorption capability. It has been reported that the functional groups, pH, and charge on the surface of nanoHAP have great effects on its surface properties.[47] Therefore, to improve the practical applications of nanoHAP as catalyst in organic synthesis, the modification surface of nanoHAP with functional groups is an effective method to obtain the unique nanoHAP properties. The use of

organophosphates, mostly alkylphosphates for surface modification of nanoHAP have been described previously.[48] It has been found that, there are strong interactions between the phosphonic groups of organophosphates with P-OH and perhaps Ca-OH groups on the surface of nanoHAP which leads to formation of $P_S$-O-P and P-O- $Ca^{2+}$ bonds.[48c] 2-Aminoethyl dihydrogen phosphate ($AEPH_2$) as a fairly unknown phospholipid and biodegradable compound can be used as a surface modification agent. $AEPH_2$ is a bifunctional organic molecule that has both a phosphate group and an amino group.[49] Therefore, the phosphate group can be used for binding to nanoHAP surface and the amino group can also work as an anchoring point for bonding of several metal ions, and other functional groups. In continuing our efforts toward the development of efficient and environmentally benign heterogeneous catalysts,[50] herein, we designed nanoHAP that is modified with $AEPH_2$ as ligand and then sulfonated with chlorosulfonic acid (HAP@$AEPH_2$-$SO_3H$) (Scheme 1). The catalytic activity of HAP@$AEPH_2$-$SO_3H$ as an eco-friendly, reusable heterogeneous catalyst was proved for the synthesis of 4,4'-( aryl methylene)bis(3-methyl-1*H*-pyrazol-5-ol)s via one-pot reaction (see Scheme 2).

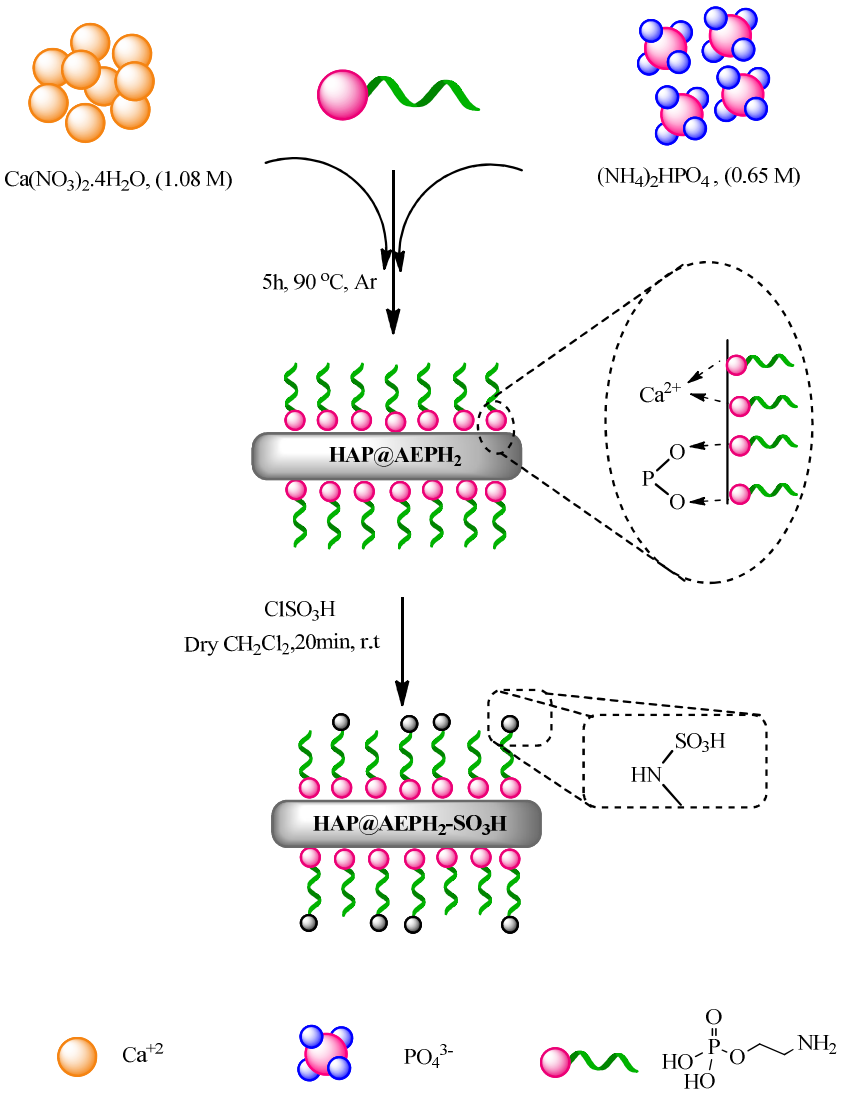


**Scheme 1** Preparation steps of HAP@AEPH$_2$-SO$_3$H.

## Results and Discussion

### Characterization of catalyst

According to the pathway shown in Scheme 1, HAP@AEPH$_2$-SO$_3$H as a novel strong and stable solid acid catalyst was synthesized. The structure and morphology of the prepared catalyst was characterized by Fourier transform infrared spectroscopy (FT-IR), thermogravimetric analysis (TGA), differential thermal analysis (DTA), scanning

electron microscopy (SEM), elemental analysis (CHN), transmission electron microscopy (TEM) and X-ray powder diffraction (XRD) which confirmed the successful preparation of the new catalyst.

In order to confirm the successful functionalization of nanoHAP with $AEPH_2$ and then with chlorosulfuric acid, FT-IR spectra of HAP@$AEPH_2$ and HAP@$AEPH_2$-$SO_3H$ were recorded (Figure 1). Figure 1a depicts the FT-IR spectrum of the nanoHAP functionalized with $AEPH_2$. As can be seen, the stretching and bending vibration of $OH^-$ ion in hydroxyapatite were detected around 3572 and 630 $cm^{-1}$ respectively. Also, the broad band at 3450-3050 $cm^{-1}$ (due to stretching vibration) and the weak band at 1637–1630 $cm^{-1}$ (due to bending vibration) were attributed to the crystal water and surface adsorbed water. Additional vibrational modes at 1098, 1031, 962, 601, 571, and 471 $cm^{-1}$ could be ascribed to the asymmetric, symmetric stretching and bending vibrations of the $PO_4^{3-}$ ions respectively.[51] In addition to the principal absorption bands of nanoHAP, appearance of two absorption bands at 2917 and 2851 $cm^{-1}$ due to asymmetric and symmetric vibrational frequencies of -$CH_2$, confirmed the successful attachment of $AEPH_2$ on the surface of the nanoHAP (Figure 1 a).[52] In FT-IR spectrum of HAP@$AEPH_2$-$SO_3H$ (Figure 1 b), the intensity of absorption band at 3450-3050 $cm^{-1}$ was increased because of the presence of more OH groups which appeared after sulfonation. Furthermore, as compared with Figure 1a, we can see some new absorption bands at 1325 and 1155 $cm^{-1}$ which are attributed to the asymmetric and symmetric stretching frequencies of S=O.[53] These absorption bands reveal that -$SO_3H$ group has been successfully grafted onto the surface of HAP@$AEPH_2$.

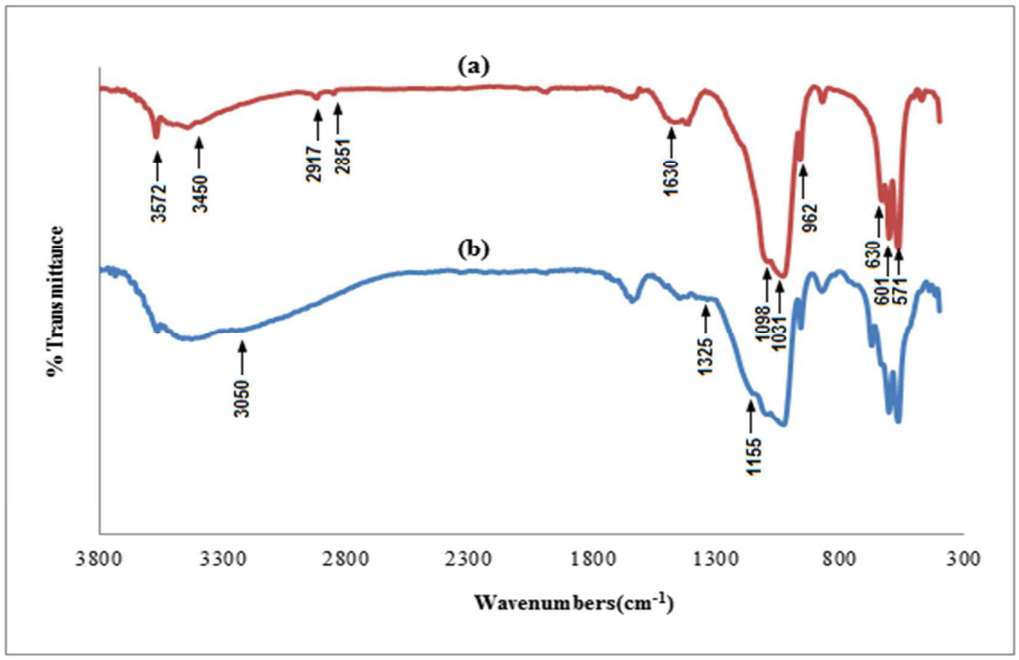


**Figure 1.** FT-IR spectrum of (a) HAP@AEPH$_2$ and (b) HAP@AEPH$_2$-SO$_3$H.

The crystallinity and phase identification of the HAP@AEPH$_2$ and HAP@AEPH$_2$-SO$_3$H were determined by using X-ray diffraction (XRD). As presented in Figure 2, the characteristic peaks with strong intensities appeared at angles corresponding to (002), (211), (300), (202), (310), (222), (213) and (004) crystallographic faces which are in agreement with the standard data of nanoHAP (JCPDS: 74-0565).[54] The XRD results also demonstrate the presence of hexagonal phase nanoHAP with high crystallinity.

Although XRD analysis of the HAP@AEPH$_2$-SO$_3$H showed no considerable broadening or shifting of peaks when compared with the XRD of HAP@AEPH$_2$ (Figure 2) but an additional peak observed in the HAP@AEPH$_2$-SO$_3$H pattern at 2θ = 25.4° could be be attributed to a little impurity CaSO$_4$ due to sulfonation (JCPDS: 37-1496) (Figure 2b). [55]

In spite of this, it could be seen that the modification of the nanoHAP with $AEPH_2$ and chlorosulfuric acid did not change the crystal structure of the nanoHAP.

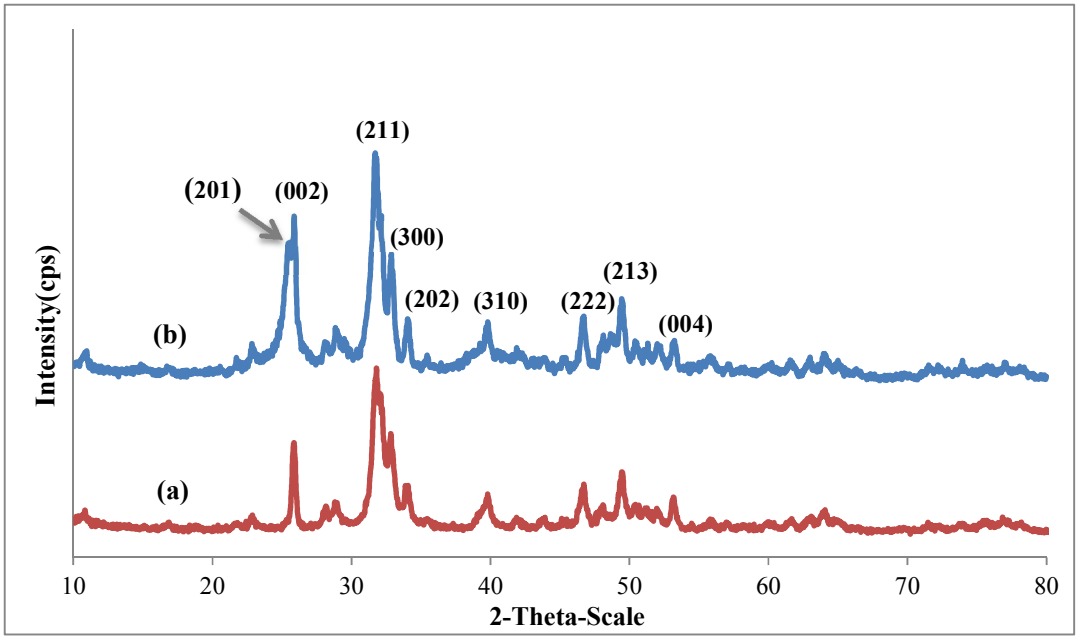


**Figure 2.** The XRD patterns of (a) HAP@$AEPH_2$ and (b) HAP@$AEPH_2$-$SO_3H$.

In addition, scanning electron microscopic and transmission electron microscopic (SEM and TEM) images were used to investigate the morphology and size of HAP@$AEPH_2$-$SO_3H$ nanoparticles. Figures 3a and 3b represent the SEM micrographs of HAP@$AEPH_2$-$SO_3H$ nanoparticles. These images demonstrate that HAP@$AEPH_2$-$SO_3H$ nanoparticles have uniform nanorods morphology which are similar to the particle morphologies reported elsewhere.[56] The TEM images of the HAP@$AEPH_2$-$SO_3H$ nanoparticles shown in Figures 3c and 3d revealed that synthesized nanoparticles are rod in shape with a mean size range of 10-100 nm. They also indicate that in comparison with literature[57] there is no change in the shape of nanoHAP after being functionalized with $AEPH_2$ and sulfonic acid and the surface morphology is also retained.

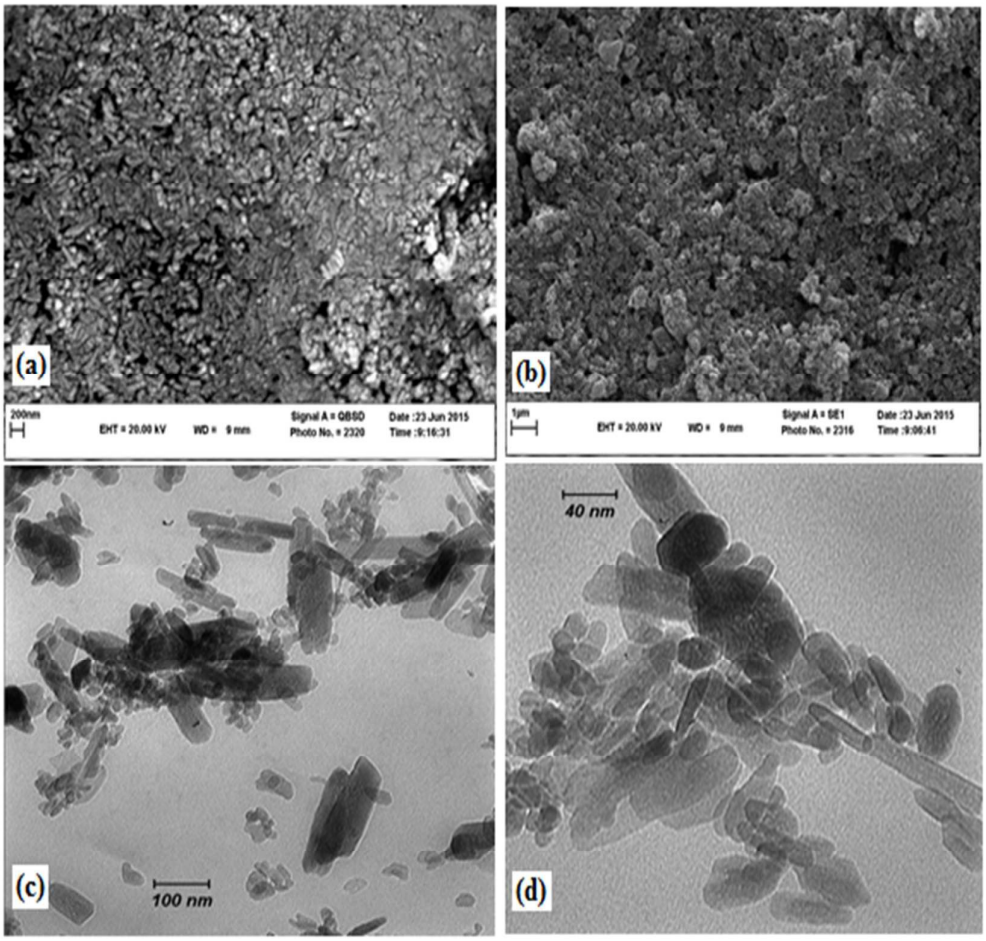


**Figure 3.** (a, b) SEM images of HAP@AEPH$_2$-SO$_3$H, (c, d) TEM images of HAP@AEPH$_2$-SO$_3$H.

Quantitative determination of the organic functional groups loaded on the surface of nanoHAP was studied by TGA and DTA (Figure 4). For HAP@AEPH$_2$, weight loss at temperatures below 200 $^{\circ}$C (4.00 %) is probably related to the physically adsorbed water on the catalyst surface. Also, the weight loss from 200 to 500$^{\circ}$C is associated with the decomposition of AEPH$_2$ groups grafted to the nanoHAP surface (Figure 4 a).[58] The TGA curve of HAP@AEPH$_2$-SO$_3$H (Figure 4 b) shows a three weight loss steps. The initial weight loss up to 200 $^{\circ}$C is due to absorbed water, second step involves the decomposition of AEPH$_2$ which started after 200 $^{\circ}$C and continued up to

500 °C. The last step can be observed between 500 °C and 850 °C, corresponding to the thermal decomposition of $SO_3H$ groups embedded via $AEPH_2$ on the surface of nanoHAP.[59]

According to the TGA curves, it can be estimated that the amount of $AEPH_2$ and sulfonic acid functionalized into the surface of catalyst are about 5.60 and 8.00 % respectively.

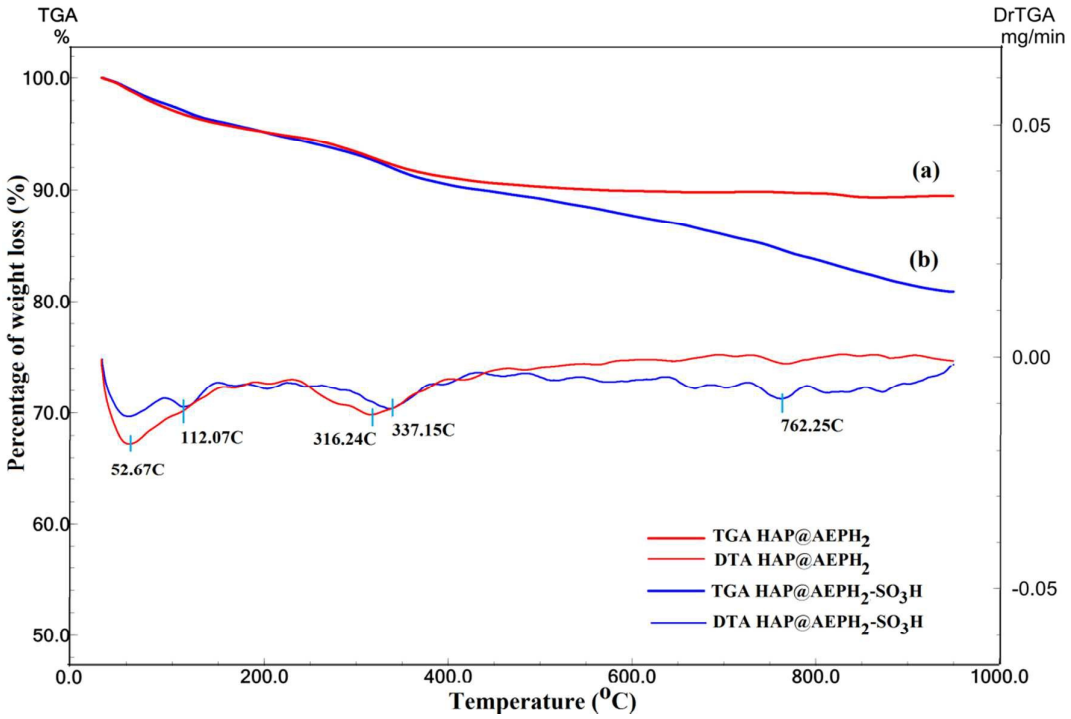


**Figure 4.** The TGA/DTA Thermograms of (a) HAP@$AEPH_2$ (b) HAP@$AEPH_2$-$SO_3H$.

In addition to the TGA/DTA analysis, the contents of $AEPH_2$ and sulfonic acid were also determined by elemental analysis (Table 1). As can be seen in Table 1, the elemental analysis of the catalyst indicated that 1.008 mmol of $AEPH_2$ and 1.040 mmol of sulfonic acid are incorporated into 1.000 g of HAP@$AEPH_2$-$SO_3H$ which is in good agreement with the data obtained from TGA.

**Table1** TGA and elemental analysis data of HAP@AEPH$_2$ and HAP@AEPH$_2$-SO$_3$H.

| Samples | TGA (%) | | | Elemental analysis (w/w %) | | |
|---|---|---|---|---|---|---|
| | $H_2O$ | $AEPH_2$ | $SO_3H$ | C | N | S |
| HAP@AEPH$_2$ | 4.000 (2.200 mmol/g) | 5.600 (1.010 mmol/g) | - | 2.409 (1.004 mmol/g) | 1.397 (1.000 mmol/g) | - |
| HAP@AEPH$_2$ -SO$_3$H | 4.000 (2.200 mmol/g) | 5.600 (1.010 mmol/g) | 8.000 (1.065 mmol/g) | 2.419 (1.008 mmol/g) | 1.409 (1.007 mmol/g) | 3.32 (1.040 mmol/g) |

Moreover, the amount of acidic sites in HAP@AEPH$_2$-SO$_3$H was determined by back-titration analysis of the catalyst: 100 mg of catalyst was added to a solution of NaOH (15 mL, 0.1 N).The resulting suspension was maintained at room temperature overnight under stirring. After that the suspension was filtered. The filtrate was neutralized by a standard solution of HCl (0.1 M). The consumed volume of HCl (14.1 mL) determined the amount of loaded NHSO$_3$H per 1.000 g of HAP@AEPH$_2$-SO$_3$H (0.900 mmol of NHSO$_3$H per 1.000 g of catalyst). This result is in good agreement with those of the results obtained from TGA and elemental analysis.

**Catalytic synthesis of 4,4'-(aryl methylene)bis(3-methyl-1*H*-pyrazol-5-ol)**

In continuation of our studies to develop the new catalysts for organic transformations[50] and to replace the conventional, toxic and polluting BrÖnsted acid catalysts with eco-friendly, reusable, heterogeneous catalysts, HAP@AEPH$_2$-SO$_3$H was used as solid acid catalyst in one-pot preparation of 4,4'-(aryl methylene)bis(3-methyl-1*H*-pyrazol-5-ol)s from phenylhydrazine/or hydrazine hydrate, ethylacetoacetate and aldehydes (Scheme 2).

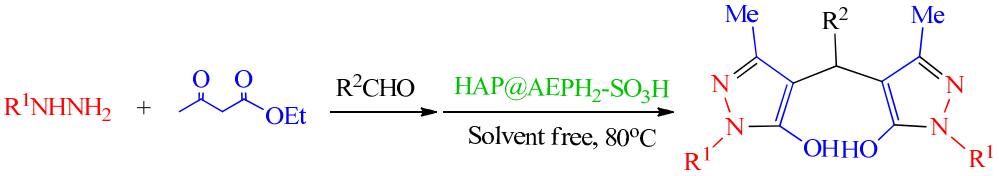


$R^1$= H, $C_6H_5$

$R^2$= $C_6H_5$, 4-(OH)$C_6H_4$, 3-(OH)$C_6H_4$, 2-(OH)$C_6H_4$, 4-(OMe)$C_6H_4$, 3-(OMe)$C_6H_4$, 4-(Me)$C_6H_4$, 3-(Me)$C_6H_4$, 5-(Br)-2-(OH)$C_6H_3$, 4-($^i$Pr)$C_6H_4$, 4-($Me_2N$)$C_6H_4$, 2- (Cl)$C_6H_4$, 4-(Cl)$C_6H_4$, 2,4-$(Cl)_2C_6H_3$, 4-(Br)$C_6H_4$, 3-($NO_2$)$C_6H_4$, 2-($NO_2$)$C_6H_4$, 1-Naphthyl, 2-Pyridyl, 3-Pyridyl, $C_6H_5$CH=CH

**Scheme 2** One-pot synthesis of 4,4'-(aryl methylene)bis(3-methyl-1*H*-pyrazol-5-ol)s catalyzed by HAP@AEP$H_2$-$SO_3H$.

To find an appropriate reaction medium for the synthesis of 4,4'-(aryl methylene)bis(3-methyl-1*H*-pyrazol-5-ol)s in the presence of a catalytic amount of HAP@AEP$H_2$-$SO_3H$, one pot reaction between phenylhydrazine (2 mmol), ethyl acetoacetate (2 mmol) and benzaldehyde (1 mmol) was selected as a model reaction. The model reaction was examined under different reaction conditions such as: different solvents, different temperatures and various amounts of catalyst (Table 2). A blank experiment without catalyst under solvent-free conditions at 80 ºC gave very low yield (10 %) after 24 h (Table 2, entry 1). The efficient catalytic activity of HAP@AEP$H_2$-$SO_3H$ was confirmed by performing the model reaction in the presence of nanoHAP and nanoHAP-$NH_2$. The desired product was scarcely obtained (20 %) in the presence of nanoHAP and nano HAP-$NH_2$ under solvent-free conditions at 80 ºC (Table 2, entries 2-3). Applying 2 mol % of HAP@AEP$H_2$-$SO_3H$ (contains 0.02 mmol of acid) under solvent-free conditions at 80 ºC produced 4,4'-(phenylmethylene)bis(3-methyl-1*H*-pyrazol-5-ol) in high yield after 2 (min) (Table 2, entry 4). We examined the effect of different temperatures on the model reaction under solvent free condition. The reactions took a long time to achieve high yield of the desired product (Table 2, entries 5-8). To evaluate the effect of different amounts

of HAP@AEPH$_2$-SO$_3$H, the model reaction was performed in the presence of 1 mol % (contains 0.01 mmol of acid) and 1.5 mol % (contains 0.015 mmol of acid) of catalyst (Table 2, entries 9-10). Best result was obtained by applying 1.5 mol % of catalyst under solvent free conditions at 80 ºC. To examine the effect of solvent, various solvents were screened ($H_2O$, EtOH, $H_2O$/EtOH (1/1) and $CH_3CN$) in the preparation of 4,4'-(phenylmethylene)bis(3-methyl-1*H*-pyrazol-5-ol) in the presence of 1.5 mol % of HAP@AEPH$_2$-SO$_3$H (Table 2, entries 11–14). It is observed that solvent-free conditions gave the best result for this transformation.

**Table 2** Synthesis of 4,4'-(phenylmethylene)bis(3-methyl-1*H*-pyrazol-5-ol) in the presence of HAP@AEPH$_2$-SO$_3$H under different reaction conditions.

| Entry | Catalyst (mol %) | Solvent | Temperature (˚C) | Time (min) | Isolated Yield (%) |
|---|---|---|---|---|---|
| 1 | - | Solvent-free | 80 | 24(h) | 10 |
| 2* | 2 | Solvent-free | 80 | 3(h) | 20 |
| 3** | 2 | Solvent-free | 80 | 3(h) | 20 |
| 4 | 2 | Solvent-free | 80 | 2 | 98 |
| 5 | 2 | Solvent-free | 70 | 6 | 92 |
| 6 | 2 | Solvent free | 60 | 10 | 94 |
| 7 | 2 | Solvent-free | 40 | 45 | 95 |
| 8 | 2 | Solvent-free | r.t | 2(h) | 45 |
| 9 | 1 | Solvent-free | 80 | 10 | 95 |
| 10 | 1.5 | Solvent-free | 80 | 3 | 98 |
| 11 | 1.5 | $H_2O$ | 80 | 10 | 75 |
| 12 | 1.5 | EtOH | 80 | 15 | 70 |
| 13 | 1.5 | $H_2O$/ EtOH (1:1) | 80 | 15 | 65 |
| 14 | 1.5 | $CH_3CN$ | 80 | 10 | 75 |

* The reaction was performed in the presence of nanoHAP.

** The reaction was performed in the presence of nanoHAP-$NH_2$.

In the next step, to explore the scope and efficiency of this one-pot reaction, with this result in hand, we examined a range of various aromatic aldehydes under the optimized reaction conditions. For this purpose, phenyl hydrazine/ or hydrazine (2 mmol), ethylacetoacetate (2 mmol) and a broad range of structurally diverse aromatic aldehydes (1 mmol) were condensed in the presence of 1.5 mol % of HAP@$AEPH_2$-$SO_3H$ to achieve the desired product. The results are summarized in Table 3. Aromatic aldehydes (bearing electron withdrawing and electron-donating groups) led to rapid formation of products 3a-3q (Table 3, entries 2-17) in high yields. Also heteroaromatic aldehydes such as pyridine carboxaldehydes, and allylic aldehydes such as cinnamaldehyde led to products 3r (94 %), 3s (93 %), and 3t (90 %) respectively (Table 3, entries 18-20).

We also used hydrazine instead of phenylhyrazine in this reaction (Table 3, entries 21-23). The desired products were also obtained rapidly in excellent yields.

**Table 3** Preparation of 4, 4′-(aryl methylene)bis(1*H*-pyrazol-5-ol)s derivatives catalyzed by HAP@$AEPH_2$-$SO_3H$ under solvent-free conditions at 80 °C.

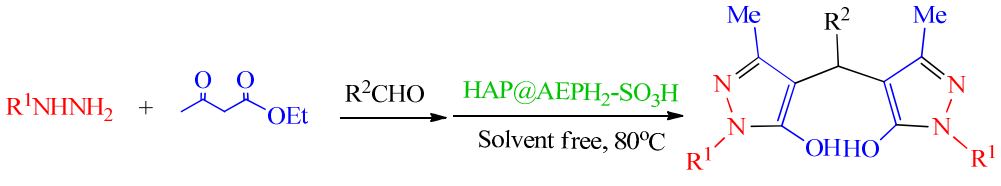


**3a-w**

| Entry | $R^1$ | $R^2$ | Product | Time (min) | Isolated Yield (%) |
|---|---|---|---|---|---|

| | | | | | |
|---|---|---|---|---|---|
| 1 | $C_6H_5$ | $C_6H_5$ | 3a | 3 | 98 |
| 2 | $C_6H_5$ | 4-$OHC_6H_4$ | 3b | 2 | 95 |
| 3 | $C_6H_5$ | 3-$OHC_6H_4$ | 3c | 3 | 93 |
| 4 | $C_6H_5$ | 2-$OHC_6H_4$ | 3d | 4 | 90 |
| 5 | $C_6H_5$ | 4-$OMeC_6H_4$ | 3e | 3 | 98 |
| 6 | $C_6H_5$ | 3-$OMeC_6H_4$ | 3f | 7 | 93 |
| 7 | $C_6H_5$ | 4-$MeC_6H_4$ | 3g | 5 | 93 |
| 8 | $C_6H_5$ | 3-$MeC_6H_4$ | 3h | 7 | 85 |
| 9 | $C_6H_5$ | 5-Br-2-$OHC_6H_3$ | 3i | 7 | 92 |
| 10 | $C_6H_5$ | 4-$^{i}PrC_6H_4$ | 3j | 5 | 80 |
| 11 | $C_6H_5$ | 2-$ClC_6H_4$ | 3k | 7 | 80 |
| 12 | $C_6H_5$ | 4-$ClC_6H_4$ | 3l | 3 | 98 |
| 13 | $C_6H_5$ | 2,4-$(Cl)_2C_6H_3$ | 3m | 7 | 85 |
| 14 | $C_6H_5$ | 4-$BrC_6H_4$ | 3n | 2 | 97 |
| 15 | $C_6H_5$ | 3-$NO_2C_6H_4$ | 3o | 3 | 80 |
| 16 | $C_6H_5$ | 2-$NO_2C_6H_4$ | 3p | 5 | 80 |
| 17 | $C_6H_5$ | 1-Naphthyl | 3q | 5 | 95 |
| 18 | $C_6H_5$ | 2-Pyridyl | 3r | 2 | 94 |
| 19 | $C_6H_5$ | 3-Pyridyl | 3s | 3 | 93 |
| 20 | $C_6H_5$ | $C_6H_5CH=CH_2$ | 3t | 5 | 90 |
| 21 | H | $C_6H_5$ | 3u | 10 | 98 |
| 22 | H | 4-$ClC_6H_4$ | 3v | 8 | 98 |
| 23 | H | 4-$MeC_6H_4$ | 3w | 10 | 95 |

The structures of all synthesized compounds 3a–w have been established by their melting points, FT-IR spectroscopy and $^{1}$H NMR spectroscopy. Moreover, the selected compounds were further identified by $^{13}$C NMR spectroscopy, mass spectrometry and elemental analysis.

The FT-IR spectrum of purified products displayed characteristic signals for OH, C=N and C=C bonds around 3450-2500, 1600 and 1499 cm$^{-1}$ respectively. Also, the $^{1}$H NMR spectra exhibited a sharp singlet resonating at around 5.50-4.89 ppm due to aryl methylene proton and two broad peaks around 13.91 and 12.40 ppm revealed two –OH groups. In $^{13}$C NMR spectra, a signal at 32 ppm is assigned to aryl methylene carbon. The elemental analysis of the synthesized compounds was also in good conformity with the proposed structures.

To further elucidate the structure of products, mass spectrometry was provided. As can be seen, molecular ion was not evident in some of mass spectra because of the very facile cleavage of C-C bond between aryl methylene carbon and pyrazole ring. However, some useful fragmentation information for each compound has been described, which can be beneficial for depicted desired products.

A reasonable mechanism for the formation of 4,4′-(aryl methylene)bis(1*H*-pyrazol-5-ol)s derivatives is proposed in Scheme 3. The reaction involves the initial formation of pyrazolone (**VI**) (which is in equiblirium with its other tautomeric form (**VII**)) by the reaction between the protonated form of ethylacetoacetate (**I**) and phenyhydrazine/ or hydrazine. Afterwards in acidic media, condensation of the intermediate (**VII**) with aldehyde and subsequent dehydration, lead to formation of **IX.** A Michael addition reaction between **IX** and **VII**, produced two tautomeric forms **XI** and **XII** followed by releasing of the acidic catalyst. Then the solid acid catalyst re-enters to the catalytic cycle.

Among various reactions, we found that in the reaction between 4-$Me_2N$-$C_6H_4$-CHO and 3-methyl-1-phenyl-1*H*-pyrazol-5-ol (**VII**), no desired product was obtained. Instead, (*E*)-4-(4-(dimethylamino)benzylidene)-3-methyl-1-phenyl-1*H*-pyrazol-5(4*H*)-one as product was formed, which was established by FT-IR, mass spectrum and $^1$H NMR spectrum (see supporting information ) (Scheme 3). This effect can be explained by conjugative effect that is responsible for greater stability as compared to its analogues (formed by use of other aldehydes).[60]

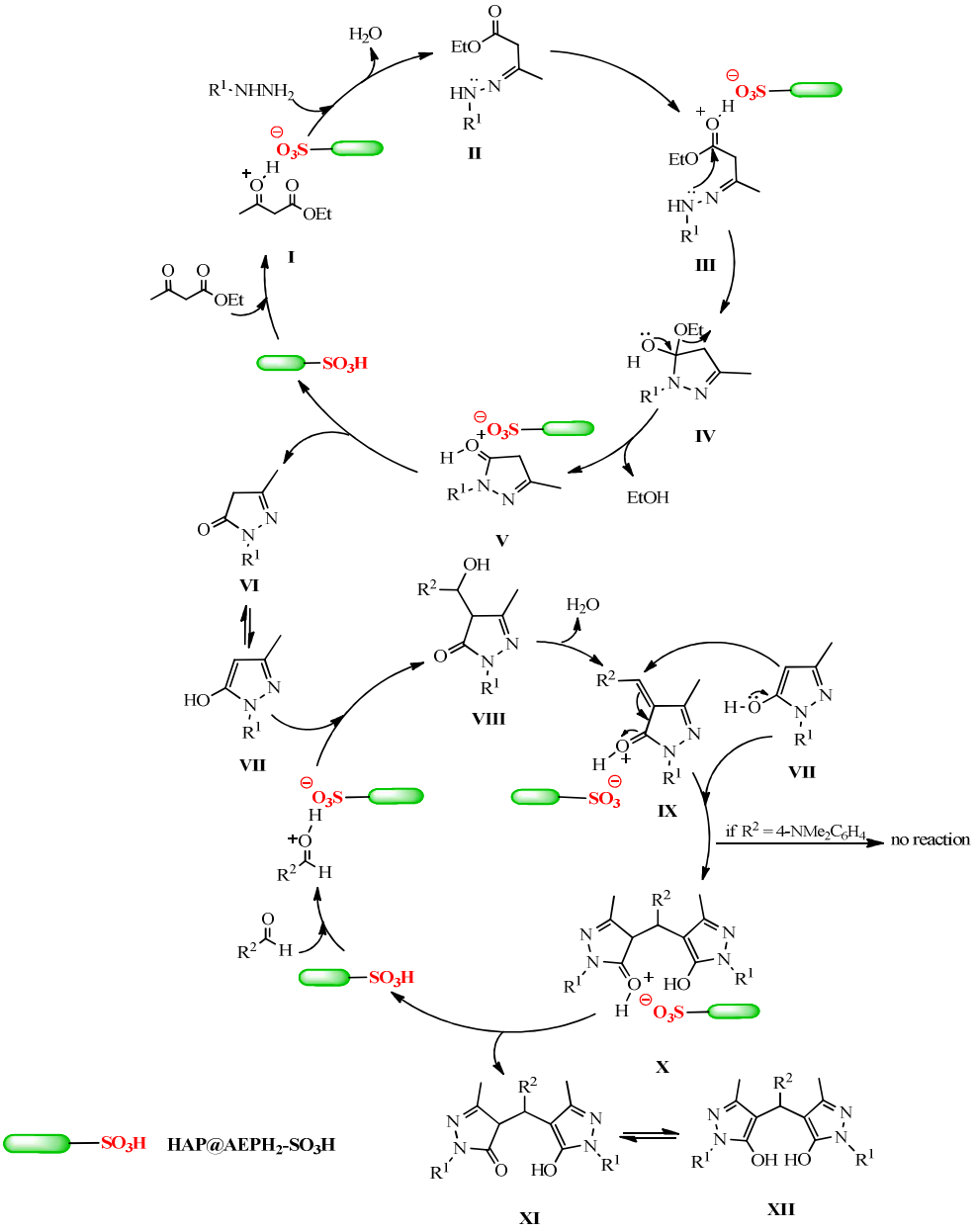

**Scheme 3** Proposed mechanism for the synthesis of 4,4'-(aryl methylene)bis(3-methyl-1*H*-pyrazol-5-ol)s using solid acid catalyst (HAP@AEPH$_2$-SO$_3$H).

In another study, the reusability of the catalyst that is one of the most important benefits and makes it useful for commercial applications was examined upon model reaction. In this experiment, after completion the reaction, the reaction mixture was boiled in EtOAc and then centrifuged to separate the catalyst. To remove all organic compounds, the catalyst was refluxed in EtOAc (3×10) and centrifuged consecutively. The recycled catalyst was dried at 50 ºC under vacuum for 3 h and used in the next run of the model reaction. The results of this experiment and five subsequent experiments were almost consistent in yields (97, 97, 94, 92, 85 %). Although slightly more time was required to complete the reaction in the fifth run, the yields are comparable to those seen earlier (Figure 5). Elemental analysis of reused catalyst (C 2.398 %, N 1.368 %, S 3.101 %) showed that there was no significant leaching of ligand AEPH$_2$ from catalyst to the reaction mixture but a little leaching SO$_3$H can be observed away from the surface of catalyst after five runs of reaction.

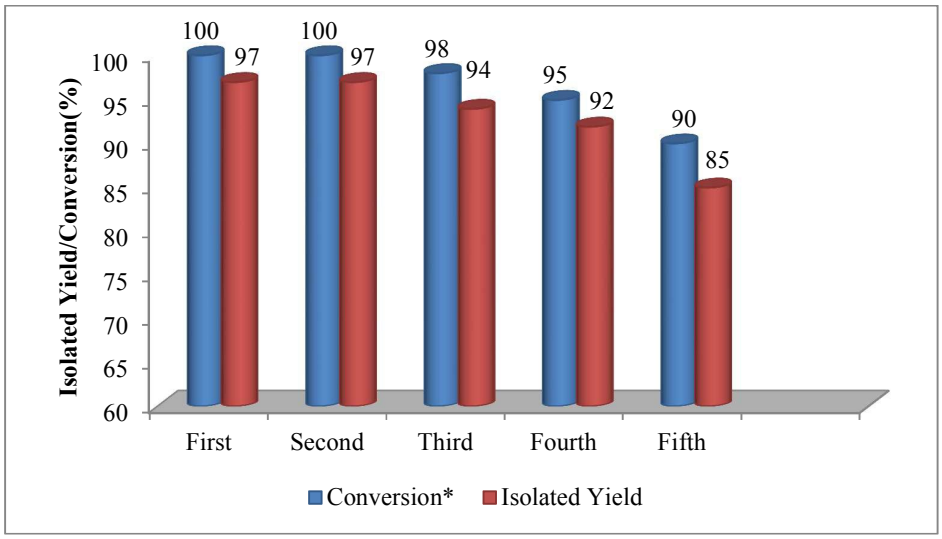

**Figure 5.** Synthesis of 4,4'-(phenylmethylene)bis(3-methyl-1*H*-pyrazol-5-ol) in the presence of reused HAP@AEPH$_2$-SO$_3$H.

*The data referred to conversion of benzaldehyde.

We compared the efficiency of HAP@AEPH$_2$-SO$_3$H with the previously reported catalysts in literature which applied in one-pot preparation of 4,4′-(aryl methylene)bis(1*H*-pyrazol-5-ol)s derivatives. The results are shown in Table 4. It is clear from Table 4 that HAP@AEPH$_2$-SO$_3$H promoted the reaction more effectively than a number of other catalysts, particularly in terms of the reaction yield and also the time required to complete the reaction.

**Table 4** Comparison efficiency of various catalysts in the synthesis of 4,4'-( aryl methylene)bis(3-methyl-1*H*-pyrazol-5-ol)s via one-pot reaction.

| Entry | Catalyst | Solvent | Temperature (°C) | Time (min) | Yield (%) | Reference |
|---|---|---|---|---|---|---|
| 1 | Ultrasonic irradiation | H$_2$O/EtOH(1:1) | R.T | 15 | 98 | 45 |
| 2 | 2-HEAP* | Solvent-free | 90 | 30 | 91 | 47 |
| 3 | SBPPSA** | Solvent-free | 80 | 45 | 93 | 42 |
| 4 | RHA-SO$_3$H | Solvent-free | 80 | 3 | 91 | 46 |
| 5 | DCDBTSD*** | Solvent-free | 80 | 100 | 74 | 44 |
| 6 | HAP@AEPH$_2$-SO$_3$H | Solvent-free | 80 | 3 | 98 | Present study |

* 2-Hydroxy ethylammonium propionate (2-HEAP)

** Silica-bonded N-propylpiperazine sulfamic acid (SBPPSA)

[***]N, 2-Dibromo-6-chloro-3,4-dihydro-2*H* benzo[e][1,2,4]thiadiazine-7-sulfonamide 1,1-dioxide (DCDBTSD)

## Experimental

### *General*

The purity determinations of the products were accomplished by TLC on silica gel polygram STL G/UV 254 plates. The melting points of products were determined with an Electrothermal Type 9100 melting point apparatus. The FTIR spectra were recorded on pressed KBr pellets using a AVATAR 370 FT-IR spectrometer (Therma Nicolet spectrometer, USA) at room temperature in the range between 4000 and 400 $cm^{-1}$ with a resolution of 4 $cm^{-1}$, and each spectrum was the average of 32 scans. NMR spectra were recorded on a NMR Bruker Avance spectrometer at 400 and 300 MHz in DMSO-$d_6$ as solvent in the presence of tetramethylsilane as internal standard. Elemental analysis was performed using a Thermo Finnigan Flash EA 1112 Series instrument (Furnace: 900 $^oC$, Oven: 65 $^oC$, Flow Carrier: 140 mL/min, Flow Referece: 100 mL/min). Mass spectra were recorded with a CH7A Varianmat Bremem instrument at 70 eV electron impact ionization, in *m/z* (rel %). TGA and DTA analysis were performed using a Shimadzu Thermogavimetric Analyzer (TG-50) in the temperature range of 25-900 ºC at a heating rate of 10 ºC /min under air atmosphere. SEM images were recorded using Leo 1450 VP scanning electron microscope operating at an acceleration voltage 20 kV, resolution of about 2 nm, image with a magnification of 20 to 300,000 times (LEO, Germany). Transmission electron microscopy (TEM) was performed with a Leo 912 AB microscope (Zeiss, Germany) with an accelerating voltage of 120 kV, image with a magnification of 80 to 500,000 times, equipped with a high resolution CCD Camera. The crystal structure of catalyst

was analyzed by XRD using a D8 ADVANCE –Bruker diffractometer operated at 40 kV and 30 mA utilizing Cu*Ka* radiation (λ= 0.154 Aº), at a step size of 0.040 º and step time of 1.5 s. The diffraction angles (2θ) were scanned from 10 º to 80 º. All yields refer to isolated products after purification by recrystallization.

**Preparation of nanoHAP functionalized with $AEPH_2$ (HAP@$AEPH_2$)**

To a solution of $Ca(NO_3)_2.4\ H_2O$ (50 mL, 1.08 M, at pH adjusted to 10 with $NH_4OH$ ) in a three-necked 500 mL round-bottomed flask equipped with condenser, argon gas inlet tube and dropping funnel, solution of $(NH_4)_2HPO_4$ (50 mL, 0.65 M at pH adjusted to 10 with $NH_4OH$) was added at 90 °C with stirring. $AEPH_2$ (0.8 g, 5 mmol) was added to the resulting suspension. The precipitate was maintained in contact with the reaction solution for 5 h at 90 °C under stirring. Then suspension was centrifuged at 10,000 rpm for 10 min and repeatedly washed with $CO_2$-free distilled water (3 × 20 mL). The product **(**nanoHAP functionalized with $AEPH_2$) was dried at 50 °C overnight. [48d]

**Preparation of HAP@$AEPH_2$-$SO_3H$**

To a magnetically stirred mixture of HAP@$AEPH_2$ (1 g) in 20 mL of dry dichloromethane, 0.5 mL (0.75 mmol) of chlorosulfuric acid was added drop by drop at room temperature. After 20 min the suspension was filtered and washed with 20 mL of dichloromethane and dried at room temperature to afford HAP@$AEPH_2$-$SO_3H$ as a white powder.

**Typical procedure for preparation of 4,4'-(phenylmethylene)bis(3-methyl-1 phenyl-1*H*-pyrazol-5-ol)**

Phenylhydrazine (2 mmol, 0.216 g) was added to a mixture of HAP@$AEPH_2$-$SO_3H$ (1.5 mol %, 0.015 g) and ethyl acetoacetate (2 mmol, 0.260 g) at 80 °C. The resultant

mixture was stirred for 1 min. Then, benzaldehyde (1 mmol, 0.106 g) was added to the reaction mixture at 80 °C. The viscose mixture was stirred vigorously for the appropriate time (5 min). Progress of the reaction was monitored by thin layer chromatography (TLC). After completion of the reaction, the reaction mixture was washed with hot ethanol (2 × 5 mL) .The resultant hot suspension was filtered off. The filtrate was cooled and the crude product was precipitated. The crude products were purified by recrystallization from ethanol (0.427 g, 98 %). To recycle the catalyst, the precipitate ( HAP@AEPH$_2$-SO$_3$H) was boiled in EtOAc (5 mL) for 10 min and then centrifuged at 10,000 rpm for 5 min. To remove all organic compounds, the catalyst was refluxed in EtOAc (3×10) for 30 min and centrifuged consecutively. The recycled catalyst was dried at 50 ºC under vacuum for 3 h and used in the next run of the model reaction.

**Spectral data**

**4,4'-(Phenylmethylene)bis(3-methyl-1-phenyl-1*H*-pyrazol-5-ol) (3a)**. [61] White cream solid; Yield 97 %; mp 170-173 °C; FT-IR (KBr): $\nu_{max}$ /cm$^{-1}$ 3058, 3031, 2921, 2553 (OH), 1730, 1599 (C=N),1497, 1449 (C=C), 1412, 1368, 1313, 1263, 1127, 1029, 857, 792, 754, 693, 596, 506, 449; $^1$H NMR (300 MHz, DMSO-$d_6$, ppm) δ 2.33 (s, 6 H, 2 CH$_3$), 4.98 (s, 1 H, C H), 7.18 –7.27 (m, 7 H, Ph), 7.45 (t, $J$ = 7.8 Hz, 4 H, Ph), 7.72 (d, $J$ = 8.1 Hz, 4 H, Ph), 13.96 (br., 1 H, OH); $^{13}$C NMR (75 MHz, DMSO-$d_6$ ppm) δ 12.1, 33.5, 120.9, 126.0, 126.3, 127.6, 128.6, 129.0, 129.4, 137.7, 142.6, 146.8; MS, *m/z* (%): 259 [M$^+$-177], 183 [M$^+$-251], 172 [M$^+$-264].

**4,4'-((4-Hydroxyphenyl)methylene)bis(3-methyl-1-phenyl-1*H*-pyrazol-5-ol) (3b)**. [62] Yellow solid; Yield 95 %; mp 159-162 °C; FT-IR (KBr) $\nu_{max}$ /cm$^{-1}$ 3145 (OH), 3068, 2921, 2774, 2663, 2582 (OH), 1600 (C=N), 1580, 1504, 1454 (C=C), 1371, 1275, 1245, 1173, 1111, 1029, 867, 816, 779, 749, 690, 583, 498, 453; $^1$H NMR (300

MHz, DMSO-$d_6$, ppm) δ 2.31 (s, 6 H, 2 $CH_3$), 4.87 (s, 1 H, CH), 6.68 (d, $J$ = 8.7 Hz, 2 H, Ph), 7.06 (d, $J$ = 8.4 Hz, 2 H, Ph), 7.25 (t, $J$ = 7.2 Hz, 2 H, Ph), 7.45 (t, $J$ = 7.8 Hz, 4 H, Ph), 7.72 (d, $J$ = 7.8 Hz, 4 H, Ph), 9.21 (s, 1 H, OH), 13.95 (br, 1 H, OH); $^{13}$C NMR (75 MHz, DMSO-$d_6$ ppm) δ 19.0, 32.8, 105.7, 115.3, 120.9, 126.0, 128.5, 129.0, 129.3, 132.7, 137.8, 146.6, 155.8, 155.9; Anal. Calcd for $C_{27}H_{24}N_4O_3$: C, 71.67; H, 5.35; N, 12.38. Found: C, 70.71; H, 5.8; N, 11.62 %; MS, *m/z* (%): 275 [$M^+$-177], 184 [$M^+$-268], 173 [$M^+$-279].

**4,4'-((3-Hydroxyphenyl)methylene)bis(3-methyl-1-phenyl-1*H*-pyrazol-5-ol) (3c).** [33b] White solid; Yield 93 %; mp 165-167 °C; IR (KBr) $\nu_{max}$ /cm$^{-1}$ 3421 (OH), 3072, 2925, 1708, 1597 (C=N), 1498 (C=C), 1455, 1405, 1368, 1284, 1155, 1029, 996, 754, 692, 503, 412; $^1$H NMR (300 MHz, DMSO-$d_6$, ppm) δ 2.32 (s, 6 H, 2 $CH_3$), 4.89 (s, 1 H, CH), 6.58 (d, $J$ = 7.8 Hz, 1 H, Ph), 6.65-6.70 (m, 2 H, Ph), 7.07 (t, $J$ = 7.8 Hz, 1 H, Ph), 7.26 (t, $J$ = 7.8 Hz, 2 H, Ph), 7.46 (t, $J$ = 7.8 Hz, 4 H, Ph), 7.73 (d, $J$ = 7.8 Hz, 4 H, Ph), 9.26 (s, 1H, OH), 13.98 (br, 1H, OH); $^{13}$C NMR (75 MHz, DMSO-$d_6$ ppm) δ 12.0, 33.4, 113.3, 114.6, 118.3, 118.8, 120.9, 126.0, 129.4, 129.4, 137.5, 138.1, 144.0, 146.8, 157.6.

**4,4'-((2-Hydroxyphenyl)methylene)bis(3-methyl-1-phenyl-1*H*-pyrazol-5-ol) (3d)**. [17] White solid; Yield 90 %; mp 228-231 °C; IR (KBr) $\nu_{max}$ /cm$^{-1}$ 3411 (OH), 3072, 2921, 2802, 2700, 2561 (OH), 1687, 1597 (C=N), 1574, 1499 (C=C), 1454, 1367, 1286, 1217, 1119, 1041, 912, 879, 847, 751, 687, 606, 586, 506, 440; $^1$H NMR (300 MHz, DMSO-$d_6$, ppm) δ 2.29 (s, 6 H, 2 $CH_3$), 5.18 (s, 1 H, CH), 6.69-6.77 (m, 2 H, Ph), 6.96-7.02 (m, 1 H, Ph), 7.23-7.27 (m, 2 H, Ph), 7.44 (t, $J$= 7.5 Hz, 4 H, Ph), 7.55 (d, $J$= 7.2 Hz, 1 H, Ph), 7.70 (d, $J$= 8.1 Hz, 4 H, Ph), 12.34 (br, 1 H, OH); MS, *m/z* (%): 275 [$M^+$-177], 256 [$M^+$-196], 173 [$M^+$-279].

**4,4'-((4-Methoxyphenyl)methylene)bis(3-methyl-1-phenyl-1*H*-pyrazol-5-ol)) (3e)**. [63] Yellow solid; Yield 90 %; mp 174-176 °C; FT-IR (KBr) $\nu_{max}$ /cm$^{-1}$ 3068, 2974, 2921, 2839, 2610, 1801, 1601 (C=N), 1581, 1507, 1459 (C=C), 1406, 1373, 1279, 1249, 1180, 1111, 1033, 966, 812, 751, 691, 596, 498, 442; $^1$H NMR (300 MHz, DMSO-$d_6$, ppm) δ 2.32 (s, 6 H, 2 $CH_3$), 3.71 (s, 3 H, $OCH_3$), 4.91 (s, 1 H, CH), 6.84 (d, *J* = 8.4 Hz, 2 H, Ph), 7.15-7.27 (m, 4 H, Ph),7.45 (t, *J*= 7.8 Hz, 4 H, Ph), 7.71 (d, *J*= 7.8 Hz, 4 H, Ph), 13.97 (br, 1 H, OH); $^{13}$C NMR (75 MHz, DMSO-$d_6$, ppm) δ 12.1, 32.8, 55.4, 113.9, 120.9, 126.0, 128.6, 129.3, 134.4, 146.6, 157.9; MS, *m/z* (%): 288 [M$^+$-178], 258 [M$^+$-208], 183 [M$^+$-283].

**4,4'-((3-Methoxyphenyl)methylene)bis(3-methyl-1-phenyl-1*H*-pyrazol-5-ol) (3f)**. [15] Pale yellow solid; Yield 93 %; mp 180-183 ºC; FT-IR (KBr) $\nu_{max}$ /cm$^{-1}$ 3517, 3064, 2971, 2885, 2711, 2550 (OH), 1603 (C=N), 1581, 1502, 1485 (C=C), 1405, 1364, 1311, 1274, 1188, 1129, 1042, 1004, 877, 790, 752, 693, 636, 599, 496, 453; $^1$H NMR (300 MHz, DMSO-$d_6$, ppm) δ 2.32 (s, 6 H, 2 $CH_3$), 3.69 (s, 3 H, $OCH_3$), 4.93 (s, 1 H, CH), 6.76-6.87 (m, 3 H, Ph), 7.18-7.28 (m, 3 H, Ph), 7.45 (t, *J*= 7.8 Hz, 4 H, Ph), 7.71 (d, *J*= 7.8 Hz, 4 H, Ph ), 12.27 (br, 1 H, OH), 13.98 (br, 1 H, OH); Anal. Calcd for $C_{28}H_{26}N_4O_3$: C, 72.09; H, 5.62; N, 12.01, Found: C, 71.9; H, 5.35; N, 11.9 %; MS, *m/z* (%): 289 [M$^+$-177], 259 [M$^+$-207], 184 [M$^+$-282].

**4,4'-(*p*-Tolylmethylene)bis(3-methyl-1-phenyl-1*H*-pyrazol-5-ol) (3g)**. [64] White solid; Yield 93 %; mp 198-200 °C; FT-IR (KBr) $\nu_{max}$ /cm$^{-1}$ 3043, 2958, 2922, 2859, 2500 (OH), 1809, 1736, 1600 (C=N), 1580, 1501, 1457 (C=C), 1408, 1372, 1291, 1196, 1131, 1070, 1024, 882, 802, 750, 688, 608, 592, 499, 444; $^1$H NMR (300 MHz, DMSO-$d_6$, ppm) δ 2.25 (s, 3 H, $PhCH_3$), 2.33 (s, 6 H, 2 $CH_3$), 4.93 (s, 1 H, CH), 7.08 (d, *J* = 8.1 Hz, 2 H, Ph), 7.16 (d, *J* = 7.8 Hz, 2 H, Ph), 7.25 (t, *J* = 7.5 Hz, 2 H, Ph), 7.45 (t, *J* = 7.5 Hz, 4 H, Ph), 7.72 (d, *J* = 7.5 Hz, 4 H, Ph), 13.94 (br, 1 H, OH); $^{13}$C

NMR (75 MHz, DMSO-$d_6$, ppm) δ 12.1, 21.0, 33.2, 105.2, 120.9, 126.0, 127.5, 129.1, 129.4, 135.3, 137.8, 139.5, 146.7; Anal. Calcd for $C_{28}H_{26}N_4O_2$: C, 74.67; H, 5.82; N, 12.44, Found: C, 74.31; H, 5.8; N, 12.24 %. MS, *m/z* (%): 273 [$M^+$-177], 259 [$M^+$-191], 184 [$M^+$-266].

**4,4'-(*m*-Tolylmethylene)bis(3-methyl-1-phenyl-1*H*-pyrazol-5-ol) (3h)**. [23] Yellow solid; Yield 85 %; mp 237-239 °C; FT-IR (KBr) $\nu_{max}$ /cm$^{-1}$ 3060, 2949, 2921, 2872, 2540 (OH), 1600 (C=N), 1578, 1499 (C=C), 1457, 1410, 1372, 1289, 1180, 1102, 1024, 902, 800, 752, 691, 597, 499, 442; $^1$H NMR (300 MHz, DMSO-$d_6$, ppm) δ 2.25 (s, 3 H, PhC$H_3$), 2.32 (s, 6 H, 2C$H_3$), 4.93 (s, 1 H, CH), 7.00-7.25 (m, 6 H, Ph), 7.45 (m, 4 H, Ph), 7.72 (d, *J* = 7.2 Hz, 4 H, Ph), 13.95 (br, 1 H, OH); $^{13}$C NMR (75 MHz, DMSO-$d_6$, ppm) δ 12.1, 21.7, 33.5, 120.9, 124.7, 126.0, 127.1, 128.2, 128.5, 129.4, 137.5, 142.6, 146.7; MS, *m/z* (%): 272 [$M^+$-178], 258 [$M^+$-192], 183 [$M^+$-267].

**4,4'-((5-Bromo-2-hydroxyphenyl)methylene)bis(3-methyl-1-phenyl-1*H*-pyrazol-5-ol) (3i)**. [27] White cream solid; Yield 92 %; mp 265-267 °C; FT-IR (KBr) $\nu_{max}$ /cm$^{-1}$ 3448 (OH), 3068, 2970, 2925, 2590 (OH), 1687, 1598, 1574, 1500, 1409, 1376, 1282, 1213, 1155, 1106, 902, 861, 784, 747, 669, 596, 514, 436; $^1$H NMR (400 MHz, DMSO-$d_6$, ppm) δ 2.26 (s, 6 H, 2 C$H_3$), 5.10 (s, 1 H, CH), 6.72 (d, *J*= 8.4 Hz, 1 H, Ph), 7.15 (d, *J*= 10.8 Hz, 1 H, Ph), 7.16-7.24 (m, 2 H, Ph), 7.43 (m, 4 H, Ph), 7.62-7.69 (m, 5 H, Ph); $^{13}$C NMR (75 MHz, DMSO-$d_6$, ppm) δ 12.1, 27.9, 110.3, 117.3, 121.1, 126.1, 129.4, 130.0, 131.6, 146.8, 153.7.

**4,4'-((4-Isopropylphenyl)methylene)bis(3-methyl-1-phenyl-1*H*-pyrazol-5-ol) (3j)**.[15] White solid; Yield 80 %; mp 211-213 °C; FT-IR (KBr) $\nu_{max}$ /cm$^{-1}$ 3068 (OH), 2958, 2921, 2868, 1797, 1732, 1601 (C=N), 1501, 1415 (C=C), 1371, 1286, 1184, 1025, 792, 753, 690, 600, 498, 449. $^1$H NMR (300 MHz, DMSO-$d_6$, ppm) δ 1.17 (d, *J*= 6.6 Hz, 6 H, 2 C$H_3$), 2.32 (s, 6 H, 2 C$H_3$), 2.79–2.88 (m, 1 H, CH), 4.92 (s, 1 H,

CH), 7.13-7.28 (m, 6 H, Ph), 7.45 (t, *J*= 7.5 Hz, 4 H, Ph), 7.71 (d, *J*= 7.8 Hz, 4 H, Ph), 12.37 (br, 1 H, OH), 13.97 (br, 1 H, OH); Anal. Calcd for $C_{30}H_{30}N_4O_2$: C, 75.29; H, 6.32; N, 11.71, Found: C, 75.1; H, 6.3; N, 11.53 %; MS, *m/z* (%): 301 [$M^+$-177], 258 [$M^+$-220], 184 [$M^+$-294].

**4, 4'-((2-Chlorophenyl)methylene)bis(3-methyl-1-phenyl-1*H*-pyrazol-5-ol) (3k)**. [17] White cream solid; Yield 70 %; mp 235-237 °C; FT-IR (KBr) $\nu_{max}$ /cm$^{-1}$ 3062, 2990, 2912, 2868, 2790, 2510 (OH), 1614 (C=N), 1540, 1499 (C=C), 1458, 1400, 1369, 1305, 1217, 1131, 1082, 1033, 898, 837, 792, 746, 689, 637, 568, 501; $^1$H NMR (300 MHz, DMSO-$d_6$, ppm) δ 2.30 (s, 6 H, 2$CH_3$), 5.15 (s, 1 H, CH), 7.24-7.34 (m, 4 H, Ph), 7.40-7.47 (m, 5 H, Ph), 7.68-7.79 (m, 5 H, Ph), 13.97 (br, 1 H, OH); $^{13}$C NMR (75 MHz, DMSO-$d_6$, ppm) δ 12.3, 32.1, 121.1, 126.1, 127.3, 128.5, 129.4, 129.9, 130.7, 132.3, 137.6, 139.8, 146.5; MS, *m/z* (%): 472 [$M^+$+2], 294 [$M^+$-176], 259 [$M^+$-211], 184 [$M^+$-286].

**4,4'-((4-Chlorophenyl)methylene)bis(3-methyl-1-phenyl-1*H*-pyrazol-5-ol) (3l).** [16] White cream solid; Yield 96 %; mp 214-216 °C; FT-IR (KBr) $\nu_{max}$ /cm$^{-1}$ 3060, 2974, 2917, 2549 (OH), 1805, 1736, 1600 (C=N), 1578, 1501, 1486 (C=C), 1408, 1372, 1295, 1204, 1086, 1014, 834, 810, 747, 688, 592, 599, 439; $^1$H NMR (300 MHz, DMSO-$d_6$, ppm) δ 2.33 (s, 6 H, 2 $CH_3$), 4.98 (s, 1 H, CH), 7.25-7.72 (m, 10 H, Ph), 7.71 (d, *J* = 7.8 Hz, 4 H, Ph); $^{13}$C NMR (75 MHz, DMSO-$d_6$, ppm) δ 12.0, 32.9, 104.8, 121.0, 126.1, 128.4, 129.4, 129.6, 131.0, 137.0, 137.7, 141.5, 146.7; MS, *m/z* (%): 470 [$M^+$], 292 [$M^+$-178], 259 [$M^+$-212].

**4,4'-((2,4-Dichlorophenyl)methylene)bis(3-methyl-1-phenyl-1*H*-pyrazol-5-ol) (3m)**.[18] White solid; Yield 85 %; mp 228-230 °C; FT-IR (KBr) $\nu_{max}$ /cm$^{-1}$ 3072, 2913, 2798, 2570 (OH), 1620 (C=N), 1558, 1498 (C=C), 1462, 1405, 1367, 1311, 1217, 1143, 1074, 902, 836, 790, 754, 693, 637, 571, 502; $^1$H NMR (300 MHz, DMSO-$d_6$,

ppm) δ 1.84 (s, 6 H, 2 $CH_3$), 5.59 (s, 1 H, CH), 7.17-7.45 (m, 9 H, Ph), 7.73 (d, $J$ = 7.5 Hz, 4H), 10.83 (br, 1 H, OH), 11.30 (br, 1H, OH); $^{13}$C NMR (75 MHz, DMSO-$d_6$, ppm) δ 11.7, 34.3, 105.4, 118.3, 118.5, 120.1, 124.6, 125.3, 128.6, 129.0, 129.5, 129.9, 136.1, 137.8, 163.5.

**4,4'-((4-Bromophenyl)methylene)bis(3-methyl-1-phenyl-1*H*-pyrazol-5-ol) (3n)**.[65] Yellow solid; Yield 97 %; mp 180-182 °C; FT-IR (KBr) $\nu_{max}$ /cm$^{-1}$ 3063, 2949, 2922, 2843, 2560 (OH), 1729, 1600 (C=N), 1578, 1499 (C=C), 1456, 1406, 1368, 1306, 1184, 1072, 1026, 1009, 910, 816, 753, 690, 593, 499; $^1$H NMR (400 MHz, DMSO-$d_6$, ppm) δ 2.29 (s, 6 H, 2 $CH_3$), 4.93 (s, 1 H, CH), 7.16-7.23 (m, 4 H, Ph), 7.44-7.45 (m, 6 H, Ph), 7.66-7.67 (m, 4 H, Ph).

**4,4'-((3-Nitrophenyl)methylene)bis(3-methyl-1-phenyl-1*H*-pyrazol-5-ol) (3o)**.[33b] Yellow solid; Yield 80 %; mp 146-148 °C; FT-IR (KBr) $\nu_{max}$ /cm$^{-1}$ 3113, 3076, 2925, 2872, 2712, 2510 (OH), 1785, 1748, 1600 (C=N), 1573, 1527, 1501 (C=C), 1418, 1349, 1285, 1200, 1106, 1004, 976, 861, 831, 803, 754, 691, 597, 497, 443; $^1$H NMR (300 MHz, DMSO-$d_6$, ppm) δ 2.37(s, 6H, 2 $CH_3$) 5.17 (s, 1 H, CH), 7.26 (t, $J$= 7.5 Hz, 2 H, Ph ), 7.46 (t, $J$= 7.5 Hz, 4 H, Ph ), 7.60 (t, $J$= 8.1, 1 H, Ph), 7.64-7.76 (m, 5 H, Ph), 8.08-8.10 (m, 2 H, Ph), 13.86 (br, 1 H, OH); MS, *m/z* (%): 303 [$M^+$-178], 257 [$M^+$-224], 183 [$M^+$-228].

**4, 4'-((2-Nitrophenyl)methylene)bis(3-methyl-1-phenyl-1*H*-pyrazol-5-ol) (3p)**.[32] Pale yellow solid; Yield 70 %; mp 220-222 °C; FT-IR (KBr) $\nu_{max}$ /cm$^{-1}$ 3072, 2917, 2798, 2580 (OH),1612 (C=N), 1558, 1521, 1498 (C=C), 1458, 1406, 1372, 1315, 1164, 1127, 1070, 898, 837, 788, 755, 677, 628, 567, 502; $^1$H NMR (300 MHz, DMSO-$d_6$, ppm) δ 2.26 (s, 6 H, 2 $CH_3$), 5.43 (s, 1 H, CH), 7.25-7.28 (m, 2 H, Ph), 7.42-7.47 (m, 5 H, Ph), 7.66-7.74 (m, 7 H, Ph), 13.50 (br, 1 H, OH); $^{13}$C NMR (75

MHz, DMSO-$d_6$, ppm) δ 11.9, 29.8, 121.0, 124.5, 126.1, 128.2, 129.4, 130.5, 132.3, 134.7, 137.6, 146.2, 150.0; MS, *m/z* (%): 483 [$M^+$+2], 305 [$M^+$-176], 259 [$M^+$-222].

**4,4'-(Naphthalen-1-ylmethylene)bis(3-methyl-1-phenyl-1*H*-pyrazol-5-ol) (3q)**.[64] Yellow solid; Yield 95 %; mp 208-210 °C; FT-IR (KBr) $\nu_{max}$ /$cm^{-1}$ 3056, 2917, 2573 (OH), 1609 (C=N), 1546, 1497 (C=C), 1457, 1402, 1369, 1315, 1217, 1135, 1037, 906, 829, 784, 755, 734, 689, 583, 547, 510; $^1$H NMR (400 MHz, DMSO-$d_6$, ppm) δ 2.31 (s, 6 H, 2 $CH_3$), 5.56 (s, 1 H, CH), 7.20 (m, 2 H, Ph), 7.39–7.53 (m, 7 H, Ph), 7.78–7.80 (m, 5 H, Ph), 7.86–8.02 (m, 3 H, Ph).

**4,4'-(Pyridin-2-ylmethylene)bis(3-methyl-1-phenyl-1*H*-pyrazol-5-ol) (3r)**.[33a] Pale yellow solid; Yield 94 %; mp 230-232 °C; FT-IR (KBr) $\nu_{max}$ /$cm^{-1}$ 3060, 2923, 2851, 2690 (OH), 1725, 1596 (C=N), 1498 (C=C), 1457, 1414, 1368, 1312, 1180, 1074, 1025, 833, 755, 691, 592, 502; $^1$H NMR (300 MHz, DMSO-$d_6$, ppm) δ 2.28 (s, 6 H, 2 $CH_3$), 5.10 (s, 1 H, CH), 7.24–7.74 (m, 13 H), 8.49 (d, *J* = 7.8 Hz, 1H, Py); $^{13}$C NMR (75 MHz, DMSO-$d_6$, ppm) δ 12.3, 36.9, 120.7, 122.1, 122.4, 125.8, 129.3, 137.6, 138.0, 147.1, 148.6, 161.6.

**4,4'-(Pyridin-3-ylmethylene)bis(3-methyl-1-phenyl-1*H*-pyrazol-5-ol) (3s)**.[16] Pale yellow solid; Yield 93 %; mp 237-239 °C; FT-IR (KBr) $\nu_{max}$ /$cm^{-1}$ 3060, 2982, 2917, 2581 (OH), 1602 (C=N), 1578, 1498 (C=C), 1456, 1420, 1355, 1290, 1180, 1102, 1028, 863, 800, 753, 692, 637, 592, 506; $^1$H NMR (300 MHz, DMSO-$d_6$, ppm) δ 2.34 (s, 6 H, 2 $CH_3$), 5.04 (s, 1 H, CH), 7.24 (t, *J* = 7.5 Hz, 2 H), 7.35 (dd, *J* = 7.8 Hz, *J* = 4.8 Hz, 1H), 7.44 (t, *J* = 7.5 Hz, 4 H), 7.70-7.75 (m, 5 H), 8.41 (d, *J* = 4.5 Hz, 1H, Py), 8.50 (d, *J* = 2.1 Hz, 1 H, Py); $^{13}$C NMR (75 MHz, DMSO-$d_6$, ppm) δ 12.1, 31.5, 104.2, 120.9, 123.7, 125.9, 129.0, 129.3, 135.5, 137.9, 138.5, 146.6, 147.3, 149.0, 157.5; MS, *m/z* (%): 260 [$M^+$-177], 232 [$M^+$-205], 184 [$M^+$-253].

***(E)*-4,4'-(3-Phenylprop-2-ene-1,1-diyl)bis(3-methyl-1-phenyl-1*H*-pyrazol-5-ol) (3t)**. Cream solid; Yield 70 %; mp 220-222 °C; FT-IR (KBr) $\nu_{max}$ /cm$^{-1}$ 3615, 3436, 3061, 2920, 2794, 2614 (OH), 1735, 1707, 1599 (C=N), 1499 (C=C), 1455, 1411, 1369, 1305, 1243, 1115, 1027, 906, 832, 785, 754, 691, 590, 498; $^1$H NMR (300 MHz, DMSO-$d_6$, ppm) δ 1.92 (d, *J*= 13.5 Hz, 3 H, $CH_3$), 2.08 (s, 3 H, $CH_3$), 2.83 (s, 1 H, CH), 7.14-7.50 (m, 10 H, Ph), 7.68-7.78 (m, 7 H, Ph), 13.85 (br, 1 H, OH); $^{13}$C NMR (75 MHz, DMSO-$d_6$, ppm) δ 11.2, 14.4, 32.1, 121.1, 126.1, 127.3, 128.5, 129.4, 129.9, 130.7, 132.3, 137.6, 139.8, 146.5; Anal. Calcd for $C_{29}H_{26}N_4O_2$: C, 75.30; H, 5.67; N, 12.11, Found: C, 75.26; H, 5.66; N, 12.08 %; MS, *m/z* (%): 285 [M$^+$-177], 257 [M$^+$-205], 184 [M$^+$-278].

**4,4'-(Phenylmethylene)bis(3-methyl-1*H*-pyrazol-5-ol) (3u)**:[43] White solid; Yield 98 %; mp 234-236 °C; FT-IR (KBr) $\nu_{max}$ /cm$^{-1}$ 3299, 3092, 2973, 2745, 1711, 1614 (C=N), 1525, 1492 (C=C), 1380, 1277, 1216, 1134, 1085, 1050, 995, 938, 877, 826, 774, 718, 692, 609, 570, 522, 460, 418; $^1$H NMR (300 MHz, DMSO-$d_6$, ppm) δ 2.07 (s, 6 H, 2 $CH_3$), 4.83 (s, 1 H, CH), 7.12–7.14 (m, 3 H, Ph), 7.19–7.24 (m, 2 H, Ph), 11.32 (br, 1 H, OH); MS, *m/z* (%): 283 [M$^+$], 184 [M$^+$-100], 127 [M$^+$-157].

**4,4'-((4-Chlorophenyl)methylene)bis(3-methyl-1*H*-pyrazol-5-ol) (3v)**.[66] White solid; Yield 98 %; mp 210-214 °C; FT-IR (KBr) $\nu_{max}$ /cm$^{-1}$ 3112, 2879, 2752, 1603 (C=N), 1568, 1533, 1490 (C=C), 1470, 1400, 1208, 1167, 1093, 1020, 852, 802, 766, 632, 606, 540, 505, 433, 406; $^1$H NMR (300 MHz, DMSO-$d_6$, ppm) δ 2.08 (s, 6 H, 2 $CH_3$), 4.84 (s, 1 H, CH), 7.13 (d, *J*= 8.4 Hz, 2 H, Ph), 7.28 (d, *J*= 8.4 Hz, 2 H, Ph), 11.32 (br, 1 H, OH); MS, *m/z* (%): 316 [M$^+$-2], 218 [M$^+$-100], 184 [M$^+$-134].

**4,4'-(*p*-Tolylmethylene)bis(3-methyl-1*H*-pyrazol-5-ol) (3w)**.[67] Pale yellow solid; Yield 95 %; mp 190-192 ºC; FT-IR (KBr) $\nu_{max}$ /cm$^{-1}$ 3558, 3311, 2968, 2680, 1719, 1615 (C=N), 1510, 1456 (C=C), 1379, 1286, 1208, 1122, 1085, 1048, 987, 930, 834,

791, 749, 697, 612, 521, 472, 419; $^{1}$H NMR (300 MHz, DMSO-$d_6$, ppm) δ 2.08 (s, 6 H, 2 $CH_3$), 2.24 (s, 3 H, $PhCH_3$), 4.80 (s, 1 H, CH), 7.05 (s, 4 H, Ph); $^{13}$C NMR (75 MHz, DMSO-$d_6$, ppm) δ 10.8, 19.0, 20.9, 32.7, 104.8, 127.8, 128.7, 134.6, 140.6, 161.5; Anal. calcd for $C_{16}H_{18}N_4O_2$: C, 64.41; H, 6.8; N, 18.78, Found: C, 64.02; H, 6.61; N, 18.52 %; MS, *m/z* (%): 297 [$M^+$], 199 [$M^+$-99], 184 [$M^+$-114].

***(E)*-4-(4-(dimethylamino)benzylidene)-3-methyl-1-phenyl-1*H*-pyrazol-5(4*H*)-one**.[60] Red solid; Yield 95 %; mp 234 °C; FT-IR (KBr) $\nu_{max}$ /cm$^{-1}$ 3076, 3011, 2917, 1668 (C=O), 1621, 1552, 1521, 1494, 1441, 1374, 1318, 1246, 1189, 1120, 995, 939, 812, 763, 669, 583, 538, 514; $^{1}$H NMR (300 MHz, DMSO-$d_6$, ppm) δ 2.29 (s, 3 H, $CH_3$), 3.12 (s, 6 H, 2 $NCH_3$), 6.84 (d, *J* = 7.5 Hz, 2 H), 7.16 (m, 1 H), 7.42 (m, 2 H), 7.56 (s, 1 H), 7.97 (d, *J* = 7.2 Hz, 2 H), 8.65 (d, *J* = 6.9 Hz, 2 H); Anal. Calcd for $C_{19}H_{19}N_3O$: C, 74.73; H, 6.27; N, 13.76. Found: C, 74.00; H, 6.12; N, 13.56 %; MS, *m/z* (%): 305 [$M^+$], 303 [$M^+$-2], 171 [$M^+$-128].

## Conclusion

In conclusion, we successfully synthesized the HAP@$AEPH_2$-$SO_3H$ as a new, green heterogeneous and reusable solid acid catalyst and characterized by FT-IR, XRD, SEM, TEM and TGA/DTA techniques. It was found that HAP@$AEPH_2$-$SO_3H$ particles were rod in shape with a mean size range of 10-100 nm. Moreover, characterization results depicted that the nanoHAP was well modified with $AEPH_2$ and sulfonic acid. The new heterogeneous catalyst was used as an efficient solid acid catalyst for rapid synthesis of 4,4′-(aryl methylene)bis(1*H*-pyrazol-5-ol)s derivatives via one-pot reaction of phenylhydrazine/hydrazine hydrate, ethylacetoacetate and aldehydes. The promising points of the present protocol which make this methodology a valid contribution to the existing processes in the field of 4,4′-(aryl

methylene)bis(1*H*-pyrazol-5-ol)s derivatives synthesis are efficiency, generality, excellent yields of products, short reaction time, low cost, simple experimental and isolation procedures, cleaner reaction profile and finally compliance with the green chemistry protocols.

**Acknowledgements**

The authors gratefully acknowledge the partial support of this study by Ferdowsi University of Mashhad Research Council (Grant no. p/3/29760).

## Notes and references

*Department of Chemistry, Faculty of Sciences, Ferdowsi University of Mashhad, Mashhad 9177948974, Iran.*

* *Corresponding author: Phone: +98-51-3880-5527, Fax: +98-51-3879-5457, E-mail: akhlaghinia@um.ac.ir*

**References**

1 B. N. Acharya, D. Saraswat, M. Tiwari, A. K. Shrivastava, R. Ghorpade, S. Apna and M. P. Kaushik, *Eur. J. Med. Chem*., 2010, **45**, 430-438.

2 M. Kidwai and R. J. Mohan, *J. Korean Chem. Soc*., 2004, **48**, 177-181.

3 S. Sugiura, S. Ohno, O. Ohtani, K. Izumi, T. Kitamikado, H. Asai, K. Kato, M. Hori and H. Fujimura, *J. Med. Chem*., 1977, **20**, 80-84.

4 H. Bayrak, A. Demirbas, N. Demirbas and S. A. Karaoglu, *Eur. J. Med. Chem*., 2010, **45**, 4726-4732.

5 K. H. Carlsson and I. Jurna, *Naunyn Schmiedebergs Arch. Pharmacol.,* 1987, **335**, 154-159.

6 K. Sujatha, G. Shanthi, N. P. Selvam, S. Manoharan, P. T. Perumal and M. Rajendran, *Bioorg. Med. Chem. Lett*., 2009, **19**, 4501-4503.

7 R. V. Antre, A. Cendilkumar, R. Nagarajan, D. Goli and R. J. Oswal, *J. Sci. Res*., 2012, **4**, 183-192.

8 M. Londershausen, *Pestic. Sci*., 1996, **48**, 269-292.

9 R. K. Tewari, R. K. Mishra, S. K. Srivastava and S. C. Bahel, *Pesticide. Res. J.,* 1990, **2**, 24.

10 G. Mariappan, P. B. Saha, L. Sutharson and A. Haldar, *Indian J. Chem., Sect. B: Org. Chem. Incl. Med. Chem.*, 2010, **49**, 1671.

11 W. S. Hamama, *Synth. Commun*., 2001, **31**, 1335-1345.

12 T. Ren, S. Liu, G. Li, J. Zhang, J. Guo, W. Li and L. Yang, *Spectrochim. Acta, Part A*, 2012, **97**, 167-175.

13 M. Abbasi-Tarighat, E. Shahbazi and K. Niknam, *Food Chem*., 2013, **138**, 991-997.

14 B. S. Kuarm and B. Rajitha, *Synth. Commun*., 2012, **42**, 2382-2387.

15 K. R. Phatangare, V. S. Padalkar, V. D. Gupta, V. S. Patil, P. G. Umape and N. Sekar, *Synth. Commun.*, 2012, **42**, 1349-1358.

16 K. Niknam and S. Mirzaee, *Synth. Commun*., 2011, **41**, 2403-2413.

17 S. Sobhani, A. Hasaninejad, M. F. Maleki and Z. P. Parizi, *Synth. Commun*., 2012, **42**, 2245-2255.

18 W. Wang, S. X. Wang, X. Y. Qin and J. T. Li, *Synth. Commun*., 2005, **35**, 1263-1269.

19 S. Sobhani, E. Safaei, A. Hasaninejad and S. J. Rezazadeh, *Organomet. Chem*., 2009, **694**, 3027-3031.

20 A. Hasaninejad, M. Shekouhy, A. Zare, S. M. S. Hoseini Ghattali and N. J. Golzar, *Iran. Chem. Soc.,* 2011, **8**, 411-423.

21 E. Mosaddegh, A. Hassankhani and A. J. Baghizadeh, *Chil. Chem. Soc*., 2010, **55**, 419-420.

22 M. A. Gouda and A. A. Abu-Hashem, *Green. Chem. Lett. Rev*., 2012, **5**, 203-209.

23 Z. Karimi-Jaberi, B. Pooladian, M. Moradi and E. Ghasemi, *Chin. J. Catal*., 2012, **33**, 1945-1949.

24 S. Tayebi, M. Baghernejad, D. Saberi and K. Niknam, *Chin. J. Catal*., 2011, **32**, 1477-1483.

25 Y. Hu, P. Wei, H. Zhou, P. K. OuYang and Z. C. Chen, *Chin. Chem. Lett*., 2006, **17**, 299-301.

26 S. Sobhani, R. Nasseri and M. Honarmand, *Can. J. Chem*., 2012, **90**, 798–804.

27 M. Baghernejad, K. Niknam, *Int. J. Chem.,* 2012, **4**, 52-60.

28 D. Shi, J. Chen, N. Wu, Q. Zhuang and X. Wang, *Chin. J. Org. Chem*., 2005, **25**, 405-408.

29 K. Niknam, D. Saberi, M. Sadegheyan and A. Deris, *Tetrahedron Lett*., 2010, **51**, 692-694.

30 A. Khazaei, M. A. Zolfigol, A. R. Moosavi-Zare, Z. Asgari, M. Shekouhy, A. Zare and A. Hasaninejad, *RSC Adv*., 2012, **2**, 8010-8013.

31 D. Singh and D. Singh, *J. Chem. Eng. Data.,* 1984*,* **29**, 355-356.

32 A. R. Moosavi-Zare, M. A. Zolfigol, M. Zarei, A. Zare, V. Khakyzadeh and A. Hasaninejad, *Appl. Catal A: Gen.,* 2013, **467**, 61-68.

33 (a) A. Hasaninejad, A. Zare, M. Shekouhy and N. Golzar, *Org. Prep. Proced. Int*., 2011, **43**, 131-137 ;(b) N. P. Tale, G. B. Tiwari and N. N. Karade, *Chin. Chem. Lett.,* 2011, **22**, 1415-1418 ;(c) Y. J. Bai, M. Li, J. Lu, Z. J. Wang and Z. Shi, *Chin. J. Org. Chem.,* 2004, **24**, 616-620.

34. M. N. Elinson, A. S. Dorofeev, R. F. Nasybullin and G. I. Nikishin, *Synthesis*, 2008, 1933-1937.

35 A. Domling and I. Ugi, *Angew. Chem. Int. Ed*., 2000, **39**, 3168-3210.

36 C. O. Kappe, *Eur. J. Med. Chem.* 2000, **35**, 1043-1052.

37 (a) J. Zhu and H. Bienayme, *Multicomponent Reactions*, Wiley-VCH, Weinheim, 2005; (b) W. Bannwarth and E. Felder, *Combinatorial Chemistry*, A Practical Approach, Wiley-VCH, Weinheim, 2000; (c) E. Soleimani and M. Zainali, *J. Org. Chem*., 2011, **76**, 10306-10311; (d) E. Soleimani, M. Zainali, and S. Samadi, *Tetrahedron Lett.,* 2011, **52**, 4186-4188.

38 S. Tayebi and K. Niknam, *Iran. J. Catal.,* 2012, **2**, 69-74.

39 E. Soleimani, S. Ghorbani, M. Taran and A. Sarvary, *C. R. Chimie,* 2012, **15**, 955-961.

40 A. Khazaei, F. Abbasi and A. R. Moosavi-Zare, *New J. Chem.*, 2014, **38**, 5287-5292.

41 A. Hasaninejad, M. Rasekhi Kazerooni and A. Zare, *ACS Sustain. Chem. Eng.,* 2013, **1**, 679–684.

42 M. Seddighi, F. Shirini and M. Mamaghani, *RSC Adv*., 2013, **3**, 24046-24053.

43 Z. Zhou and Y. Zhang, *Green. Chem. Lett. Rev.*, 2014, **7**, 18–23.

44 (a) D. Tejedor and F. Garcia-Tellado, *Chem. Soc. Rev.,* 2007, **36**, 484-491; (b) L. Weber, *Drug Discov. Today,* 2002, **7**, 143-147; (c) C. Hulme and V. Gore, *Curr. Med. Chem*., 2003, **10**, 51-80.

45 G. Lelais and D. W. C. MacMillan, *Aldrichimica Acta.,* 2006, **39**, 79-87.

46 M. Dabiri, P. Salehi, M. Bahramnejad and F. Sherafat, *J. Comb. Chem*., 2010, **12**, 638-642.

47 (a) A. Ethirajan, U. Ziener and K. Landfester, *Chem. Mater.,* 2009, **21,** 2218-2225; (b) S. R. Roohani, S. N. Nouri, Z. F. Lu, R. Appleyard and H. Zreiqat, *Biomaterials,* 2010, **31**, 5498–5509.

48 (a) T. Ishikawa, H. Tanaka, A. Yasukawa and K. Kandori, *J. Mater.Chem*., 1995, **5**, 1963-1967; (b) H. Tanaka, A. Yasukawa, K. Kandori, and T. Ishikawa, *Langmuir,* 1997, **13**, 821-826; (c) C. S. D'Andrea and A. Y. Fadeev, *Langmuir,* 2003, **19**, 7904-7910; (d) E. Boanini, M. Gazzano, K. Rubini and A. Bigi, *Adv. Mater.,* 2007, **19**, 2499-2502.

49 A. T. Myller, J. J. Karhe and T. T. Pakkanen, *Appl. Surf. Sci.,* 2010, **257**, 1616-1622.

50 (a) N. Razavi and B. Akhlaghinia. *RSC Adv.,* 2015, **5**, 12372-12381; (b) S.S.E. Ghodsinia and B. Akhlaghinia, *RSC Adv*., 2015, **5**, 49849-49860; (c) Z. Zarei and B. Akhlaghinia, *Chem. Pap.*, 2015, DOI: 10.1515/chempap-2015-0168; (d) M. Zarghani, B. Akhlaghinia, *Appl. Organometal. Chem*., 2015, DOI: 10.1002/aoc.3351.

51 M. G. Ma, Y. J. Zhu and J. Chang, *J. Phys. Chem. B*, 2006, **110**, 14226-14230.

52 Y. Daniels, N. Lyczko, A. Nzihou and S. D. Alexandratos, *Ind. Eng. Chem. Res.*, 2015, **54**, 585 -596.

53 A. Badiei, H. Goldooz, G. Mohammadi Ziarani, A. Abbasi, *J. Colloid Interface Sci.*, 2011, **357**, 63-69.

54 M. Sheykhan, L, Ma'mani, A, Ebrahimi, A. Heydari, *J. Mol. Catal. A: Chem.,* 2011, **335**, 253-261.

55 A. Z. Alshemary, Y. Goh, M. Akram, I. R. Razali, M. A. Kadir and R. Hussain, *Mater. Res. Bull.,* 2013, **48**, 2106–2110.

56 (a) F. Mohandes and M. Salavati-Niasari, *Mater. Sci. Eng., C,* 2014, **40**, 288-298; (b) G. E. Poinern, R. K. Brundavanam, N. Mondinos and Z. T. Jiang, *Ultrason. Sonochem.*, 2009, **16**, 469-474.

57 G. Wang, Y. Zhao, J. Tan, S. Zhu and K. Zhou, *Trans. Nonferrous Met. Soc. China.,* 2015, **25**, 490-496.

58 Y. Jiang, F. Sun, X. Y. Zhou, W. B. Kong and X. Y. Xie, *Chin. Chem. Lett.,* 2015, DOI: 10.1016/j.cclet.2015.04.035.

59 N. Ahmed, Z. N. Siddiqui, *J. Mol. Catal. A: Chem.*, 2014, **394**, 232–243.

60 A. D. Gupta, R. Pal and A. K. Mallik, *Green. Chem. Lett. Rev.*, 2014, **7**, 404-411.

61 D. H. Jani, H. S. Patel, H. Keharia and C. K. Modi, *Appl. Organometal. Chem.,* 2010, **24**, 99-111.

62 B. B. Thummar, U. P. Tarpada, and D. K. Raval, *J. Heterocyclic Chem.*, 2014**, 51**, 1740-1746.

63 F. Shirini, M. Seddighi, M. Mazloumi, M. Makhsous, M. Abedini, *J. Mol. Liq.,* 2015, **208**, 291–297.

64 M. Barge and R. Salunkhe, *RSC Adv.*, 2014, **4**, 31177-31183.

65 A. Zara, M. Merajoddin, A. R. Moosavi Zare and M. Zarei, *Chin. J. Chem.*, 2014, **35**, 85–89.

66 J. Safaei Ghomi, B. Khojastehbakht Koopaei and H. Shahbazi Alavi, *RSC Adv.*, 2014, **4**, 46106-46113.

67 A. Vafaee, A. Davoodnia and M. Pordel, *Res Chem Intermed.,* 2015, DOI: 10.1007/s11164-014-1896-y.